

Charge and Flux Noise from Nonequilibrium Quasiparticle Energy Distributions in Superconducting Qubits and Resonators

José Alberto Nava Aquino and Rogério de Sousa
*Department of Physics and Astronomy, University of Victoria,
 Victoria, British Columbia V8W 2Y2, Canada and
 Centre for Advanced Materials and Related Technology,
 University of Victoria, Victoria, British Columbia V8W 2Y2, Canada*
 (Dated: December 13, 2024)

The quasiparticle density observed in low-temperature superconducting circuits is several orders of magnitude larger than the value expected at thermal equilibrium. The tunneling of this excess of quasiparticles across Josephson junctions is recognized as one of the main loss and decoherence mechanisms in superconducting qubits. Here we propose an additional loss mechanism arising from nonequilibrium quasiparticle densities: Ohmic loss due to quasiparticles residing in superconducting wires away from the junctions. Our theory leverages the recent experimental demonstration that the excess quasiparticles are in *quasiequilibrium* [T. Connolly *et al.*, *Phys. Rev. Lett.* **132**, 217001 (2024)] and uses a generalized fluctuation-dissipation theorem to predict the amount of charge and flux noise generated by them. We show that the resulting contribution to qubit and resonator energy relaxation rate $1/T_1$ can be larger than the one due to amorphous two-level systems and comparable to the contribution from quasiparticle-tunneling. We also discuss the flux noise associated to charge noise fluctuations. For quasiparticles in quasiequilibrium the associated flux noise is logarithmic-in-frequency, giving rise to a “nearly white” contribution that is comparable to the flux noise observed in experiments. This contrasts to amorphous two-level systems, whose associated flux noise is shown to be superOhmic. In conclusion, wire-resident quasiparticles are a universal source of loss and decoherence even when the quasiparticles are far away from Josephson junctions.

I. INTRODUCTION

Superconducting (SC) qubits represent a promising pathway toward scalable quantum computing, leveraging the coherence of macroscopic quantum states [1]. A pivotal factor in their operational efficacy is maintaining quantum coherence, a challenge compounded by various decoherence mechanisms [2–7]. Among these, quasiparticles (QPs), excitations resulting from broken Cooper pairs, emerge as a concern. The presence of QPs in superconductors is known to give rise to surface resistance and Ohmic loss [8]. Their impact on SC qubits is believed to be the greatest when they tunnel across a Josephson junction (JJ), leading to energy relaxation and dephasing, thereby limiting qubit performance [9–12].

Several experiments show that a large population of nonequilibrium QPs (resident QPs) remain even at low temperatures ($k_B T \ll \Delta$), in spite of the thermal QP population being exponentially small ($\propto e^{-\Delta/k_B T}$, where Δ is the SC energy gap) [13, 14]. These nonequilibrium populations are believed to arise from external perturbations, such as stray infrared photons or ionizing radiation [15–17], posing a great challenge to qubit coherence. An additional unknown is the energy distribution for the resident QPs. A recent experiment provided evidence of *quasiequilibrium*, where QPs are in thermal equilibrium with the surrounding phonon bath despite having an out-of-equilibrium density. Therefore, even though the QPs arise from high-energy sources, rapid inelastic processes mediated by phonons restore them to a thermal-like energy distribution [18].

Current designs of SC circuits engineer junction asym-

metries in order to prevent QP tunneling across the circuit’s JJs, greatly reducing the impact of the QP tunneling mechanism [18–21].

Here we show that the Ohmic loss induced by QPs within the SC wires themselves gives rise to charge and flux noise even when the QPs are far from the junctions. We present explicit numerical calculations for capacitively coupled waveguide resonators (CPW resonators) and transmon qubits that demonstrate that resident QPs away from the junctions may give a larger contribution to energy relaxation than the one arising from dielectric loss due to two-level systems (TLSs).

The resulting charge noise generates flux fluctuations due to the self-inductance of the wires, giving rise to a flux noise background that is logarithmic in frequency. The magnitude of the predicted “nearly white flux noise background” is found to be comparable to values observed in flux-tunable qubits [22, 23].

II. QUBIT ENERGY RELAXATION RATE AND RESONATOR QUALITY FACTOR FROM CHARGE AND FLUX NOISE

The rate for energy equilibration between a qubit and a charge noise environment follows from Fermi’s golden rule,

$$\frac{1}{T_1} = \frac{1}{\hbar^2} |\langle 1 | \frac{\partial \mathcal{H}}{\partial Q} | 0 \rangle|^2 \left[\tilde{S}_Q(\Omega) + \tilde{S}_Q(-\Omega) \right]. \quad (1)$$

Here \mathcal{H} is the qubit Hamiltonian, $|0\rangle$ and $|1\rangle$ are its lowest energy eigenstates with energy difference $E_1 - E_0 \equiv \hbar\Omega$.

The operators Q and $\frac{\partial \mathcal{H}}{\partial Q}$ represent the qubit's charge and voltage operators, respectively. The impact of the environment is encoded in the charge noise spectral density,

$$\tilde{S}_Q(\omega) = \int_{-\infty}^{\infty} dt e^{i\omega t} \langle \delta Q(t) \delta Q(0) \rangle_T, \quad (2)$$

where $\delta Q(t)$ is the charge fluctuation operator for the environment and $\langle \cdot \rangle_T$ is thermal average. Here ω denotes an arbitrary frequency, in order to distinguish from the resonant frequency Ω for a qubit or resonator. While Eq. (1) shows that only noise at $\omega = \Omega$ contributes to $1/T_1$, off-resonant contributions at $\omega \neq \Omega$ give rise to phase relaxation processes contributing to $1/T_2^*$ and $1/T_2$ [24].

As an application of Eq. (1), assume the qubit can be described by a *simple harmonic LC-resonator*,

$$\mathcal{H} = \frac{Q^2}{2C} + \frac{\Phi^2}{2L}, \quad (3)$$

where C and L are the capacitance and inductance, respectively, and Φ is the flux operator, satisfying $[Q, \Phi] = i\hbar$. In this case Eq. (1) becomes

$$\frac{1}{T_1} = \frac{\omega}{2\hbar C} [\tilde{S}_Q(\Omega) + \tilde{S}_Q(-\Omega)], \quad (4)$$

with $\Omega = 1/\sqrt{LC}$. In Appendix A we show that the usual fluctuation-dissipation theorem remains valid when the environment satisfies the ‘‘quasithermal law’’ described below. The fluctuation-dissipation theorem relates charge noise to the linear response charge susceptibility $\tilde{\chi}_Q(\omega) = \langle \delta \tilde{Q}(\omega) \rangle / \delta \tilde{V}(\omega)$,

$$\tilde{S}_Q(\omega) = 2\hbar \text{Im} \{ \tilde{\chi}_Q(\omega) \} [n_B(\omega) + 1], \quad (5)$$

where $n_B(\omega) = 1/(e^{\hbar\omega/k_B T} - 1)$ is the Bose-Einstein distribution. Inserting this into Eq. (4) leads to

$$\frac{1}{T_1} = \frac{\Omega}{C} \text{Im} \{ \tilde{\chi}_Q(\Omega) \} \coth \left(\frac{\hbar\Omega}{2k_B T} \right). \quad (6)$$

At low temperatures $k_B T \ll \hbar\Omega$ the coth can be approximated by 1 leading to $1/T_1 = \Omega/Q$ where Q is the resonator quality factor,

$$\frac{1}{Q} = \frac{\text{Im} \{ \tilde{\chi}_Q(\Omega) \}}{C} \equiv \langle \tan(\delta) \rangle = \sum_i p_i \tan(\delta_i). \quad (7)$$

Here $\langle \tan(\delta) \rangle$ is the loss tangent averaged over regions i of the device according to the participation ratio p_i , which is defined as the electrical energy of region i divided by the total device electromagnetic energy.

One may also evaluate Eq. (1) for the transmon qubit, which is a slightly anharmonic *LC-resonator* with a Josephson junction playing the role of the inductor [3]. The $1/T_1$ is identical to Eq. (4) with the qubit frequency given by

$$\hbar\Omega \approx \sqrt{8E_J E_C} - E_C, \quad (8)$$

provided that $E_J \gg E_C$, where E_J and $E_C = e^2/(2C)$ are the Josephson and charging energies associated to the junction, respectively. Hence, the transmon is also well described by the quality factor Eq. (7).

We now move on to describe what is often believed to be the main contribution to resonator and transmon relaxation rate. TLSs defects are one of the main sources of charge noise in SC circuits [25, 26]. Inserting the definition of loss tangent to Eq. (5) we get the charge noise due to TLSs,

$$\tilde{S}_Q^{\text{TLS}}(\omega) = 2\hbar C \langle \tan(\delta_{\text{TLS}}) \rangle [n_B(\omega) + 1], \quad (9)$$

with the TLS loss tangent averaged over surface (S) and bulk (B) dielectric regions of the device,

$$\langle \tan(\delta_{\text{TLS}}) \rangle = [p_S \tan(\delta_{\text{TLS},0}^S) + p_B \tan(\delta_{\text{TLS},0}^B)] \times \tanh(\hbar\omega/2k_B T), \quad (10)$$

with typical amplitudes $\tan(\delta_{\text{TLS},0}^S) = 10^{-3}$ and $\tan(\delta_{\text{TLS},0}^B) = 10^{-6}$ for TLSs located in the bulk and surface regions, respectively [25, 26].

Finally, there is an alternative way of expressing Eq. (1) that warrants discussion. The presence of charge fluctuation imply associated flux fluctuation because $\Phi = L\dot{Q}$, where L is the SC wire self inductance and \dot{Q} is the associated current. As a result $\delta\Phi = -i\omega L\delta\tilde{Q}$, implying the flux noise spectral density $\tilde{S}_\Phi(\omega) = (L\omega)^2 \tilde{S}_Q(\omega)$ is always associated to charge noise. In this case Eq. (1) can be rewritten as

$$\frac{1}{T_1} = \frac{1}{\hbar^2} |\langle 1 | \frac{\partial \mathcal{H}}{\partial \Phi} | 0 \rangle|^2 [\tilde{S}_\Phi(\Omega) + \tilde{S}_\Phi(-\Omega)]. \quad (11)$$

It must be emphasized that if the origin of flux noise is charge fluctuation, then Eqs. (1) and (11) describe the same mechanism and should not be added together. However, Eq. (11) can be used to account for additional mechanisms not associated to charge fluctuation, e.g. flux noise due to spin-impurity fluctuation [7].

III. CHARGE SUSCEPTIBILITY AND CONDUCTIVITY FROM QUASIPARTICLES

In this section we propose analytical approximations for the charge susceptibility in a superconducting circuit and the conductivity of its quasiparticle excitations. The linear response in a general circuit due to a small perturbation in voltage V is $\delta\tilde{V} = Z\langle\delta\tilde{I}\rangle = -i\omega Z\langle\delta\tilde{Q}\rangle$, where Z is a complex impedance. The charge susceptibility in a circuit is thus $\tilde{\chi}_Q(\omega) = \frac{\langle\delta\tilde{Q}\rangle}{\delta\tilde{V}} = -\frac{1}{i\omega Z}$. Consider the circuit to be a wire made of segments of the same material, each with length ℓ_j and cross-sectional area A_j . The impedance of the wire will be given by

$$Z(\omega) = \frac{1}{\sigma(\omega)} \sum_j \frac{\ell_j}{A_j}, \quad (12)$$

where $\sigma(\omega) = \sigma_1(\omega) + i\sigma_2(\omega)$ is the SC's complex conductivity, that is affected by the presence of QPs.

The charge susceptibility due to the presence of QPs in a single compound wire is $\tilde{\chi}_Q(\omega) = \frac{i\sigma(\omega)}{\omega} \left(\sum_j \frac{\ell_j}{A_j} \right)^{-1}$ and its imaginary part for a device is

$$\text{Im} \{ \tilde{\chi}_Q(\omega) \} = \sum_{\text{disc.wires}} \frac{\sigma_1(\omega)}{\omega} \left(\sum_j \frac{\ell_j}{A_j} \right)^{-1}, \quad (13)$$

where the first sum runs over the set of wires that are disconnected (e.g. by a Josephson junction), and the second sum runs over the segments of each connected wire. Exactly the same Eq. (13) is obtained by assuming each SC wire is an inductor in parallel with a resistor containing several wire segments in series, each with resistance $R_{j,\text{QP}} = \ell_j / (A_j \sigma_1)$.

The frequency-dependent conductivities of a Bardeen-Cooper-Schrieffer (BCS) superconductor were calculated by Mattis and Bardeen in [8] for the case where the quasiparticles are at thermal equilibrium, with average occupation given by Fermi-Dirac functions $f(E) = 1/(e^{E/k_B T} + 1)$. Here $E \equiv E_k = \sqrt{\xi_k^2 + \Delta^2}$ is the BCS quasiparticle energy, with $\xi_k = \epsilon_k - \epsilon_F$ the free electron energy measured from the Fermi level ϵ_F .

The Mattis-Bardeen theory can be generalized to the case away from thermal equilibrium, provided that quasiparticle occupation remains a function of QP energy E . We shall make this key *QP energy distribution assumption* and refer to the quasiparticle occupations as $n(E)$, a function that can differ from the equilibrium Fermi-Dirac function $f(E)$. The Mattis-Bardeen conductivities then become

$$\frac{\sigma_1}{\sigma_N} = \frac{2}{\hbar\omega} \int_{\Delta}^{\infty} dE \frac{E(E + \hbar\omega) + \Delta^2}{\sqrt{E^2 - \Delta^2} \sqrt{(E + \hbar\omega)^2 - \Delta^2}} \times [n(E) - n(E + \hbar\omega)], \quad (14a)$$

$$\frac{\sigma_2}{\sigma_N} = \frac{1}{\hbar\omega} \int_{\Delta - \hbar\omega}^{\Delta} dE \frac{E(E + \hbar\omega) + \Delta^2}{\sqrt{\Delta^2 - E^2} \sqrt{(E + \hbar\omega)^2 - \Delta^2}} \times [1 - 2n(E + \hbar\omega)]. \quad (14b)$$

These expressions are valid at subgap frequencies $\hbar\omega < 2\Delta$, with σ_N the non-SC (normal state) real part of the conductivity.

In order to connect to experiments, it is fruitful to express $\sigma_1(\omega)$ in terms of the number of QPs divided by the number of electrons bound as Cooper pairs [10, 11, 27],

$$x_{\text{QP}} = \frac{N_{\text{QP}}}{2\rho\Delta} = \frac{1}{\Delta} \int_{-\infty}^{\infty} d\xi n(\sqrt{\xi^2 + \Delta^2}), \quad (15)$$

where ρ is the electron energy density near ϵ_F . As we shall argue below, the QP occupation appears to follow a ‘‘quasithermal’’ law $n(E) \approx n_0 e^{-E/k_B T}$ in experiments. Here n_0 does not depend on QP energy E or frequency

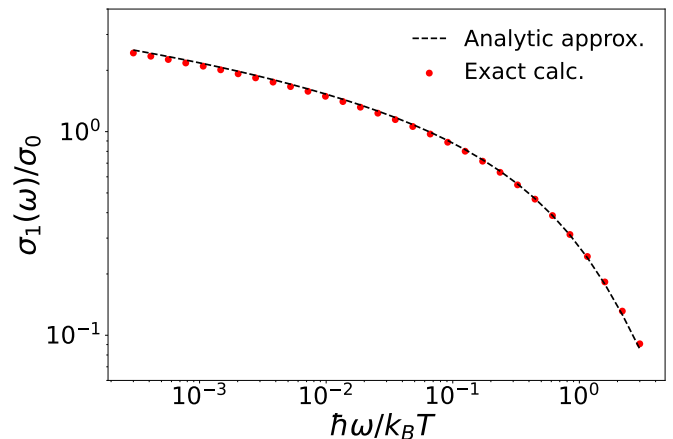


FIG. 1. Numerical calculation of $\sigma_1(\omega)$ assuming the quasithermal law for the QP distribution observed in experiments, $n(E) \propto e^{-E/k_B T}$. The plot is normalized by $\sigma_0 = \sigma_N x_{\text{QP}} (2\Delta/k_B T)^{3/2}$. In the low frequency range $\hbar\omega \lesssim k_B T$, σ_1 decreases logarithmically with increasing ω ; in the high frequency range it decreases as a power law. When $k_B T \lesssim 0.1\Delta$ we find that the exact numerical result (red points) is well approximated by the analytical expression Eq. (17) (shown as a solid line for comparison).

ω , but it may depend on other parameters such as temperature T and gap Δ . For the special case of thermal equilibrium we get $n_0 = 1$, as can be seen from $n(E) = f(E) = 1/(e^{E/k_B T} + 1) \approx e^{-E/k_B T}$. When the quasithermal law is followed and $k_B T \ll \Delta$, the QP density of states can be expanded around its singularity at $E = \Delta$: $E/\sqrt{E^2 - \Delta^2} \approx \sqrt{\Delta/[2(E - \Delta)]}$. Under this approximation we get

$$x_{\text{QP}} \approx \sqrt{2} \int_0^{\infty} dx \frac{n((1+x)\Delta)}{\sqrt{x}} = n_0 \sqrt{\frac{2\pi k_B T}{\Delta}} e^{-\frac{\Delta}{k_B T}}. \quad (16)$$

When both $\hbar\omega$ and $k_B T$ are much smaller than Δ , the conductivity is also dominated by the singularity in the QP density of states; as a result, the same approximation as in Eq. (16) leads to the following analytic approximation for the real part of the conductivity:

$$\frac{\sigma_1}{\sigma_N} \approx x_{\text{QP}} \left(\frac{2\Delta}{k_B T} \right)^{3/2} \frac{1}{\sqrt{\pi}} \left(\frac{k_B T}{\hbar\omega} \right) \sinh \left(\frac{\hbar\omega}{2k_B T} \right) \times K_0 \left(\frac{\hbar\omega}{2k_B T} \right), \quad (17)$$

where $K_0(y)$ is the modified Bessel function of the second kind.

Fig. 1 compares Eq. (17) to exact numerical integration of both Eqs. (14a) and (15), assuming the quasithermal law and $k_B T/\Delta = 0.1$. We find that Eq. (17) approximates the exact result quite well provided that $\hbar\omega, k_B T \lesssim 0.1\Delta$.

Thus, the behaviour of $\sigma_1(\omega)$ depends critically on the value of frequency relative to the thermal frequency

$k_B T / \hbar$. In the low frequency regime of $\hbar\omega \ll k_B T$, σ_1 is logarithmic in frequency as

$$\frac{\sigma_1}{\sigma_N} \approx \frac{1}{2\sqrt{\pi}} x_{\text{QP}} \left(\frac{2\Delta}{k_B T} \right)^{3/2} \left[\ln \left(\frac{4k_B T}{\hbar\omega} \right) - \gamma_E \right], \quad (18)$$

where $\gamma_E = 0.5772\dots$ is the Euler-Mascheroni constant. In the opposite high-frequency regime of $\hbar\omega \gg k_B T$, σ_1 is instead a power law,

$$\frac{\sigma_1}{\sigma_N} \approx \frac{1}{2} x_{\text{QP}} \left(\frac{2\Delta}{\hbar\omega} \right)^{3/2}. \quad (19)$$

The imaginary part of σ has even simpler behaviour, because when $k_B T \ll \Delta$ we may assume $[1 - 2n(E + \hbar\omega)] \approx 1$ in Eq. (14b). Thus when $\hbar\omega, k_B T \ll \Delta$, we can integrate Eq. (14b) analytically to obtain

$$\frac{\sigma_2}{\sigma_N} \approx \frac{\pi\Delta}{\hbar\omega}. \quad (20)$$

This agrees qualitatively with the phenomenological London theory, which leads to $\sigma_2^{\text{London}} = \frac{1}{\mu_0 \lambda^2 \omega}$ where μ_0 is the permeability of vacuum and λ is the penetration depth. We note that penetration depth λ is often measured using this London expression [28]. Therefore, it makes sense to equate σ_2^{London} to Eq. (20) in order to obtain

$$\sigma_N = \frac{\hbar}{\mu_0 \lambda^2 \pi \Delta}. \quad (21)$$

This relation, valid for $\hbar\omega, k_B T \ll \Delta$, provides a practical method for computing σ_N .

Finally, the impedance generated by QPs can be interpreted as kinetic inductance defined by $L_k = \text{Re} \left\{ \frac{iZ}{\omega} \right\}$. The kinetic inductance due to QPs residing in a wire is then $L_k = -\text{Im} \left\{ \frac{1}{\omega \sigma(\omega)} \right\} \sum_j \frac{\ell_j}{A_j} \approx \frac{1}{\omega \sigma_2(\omega)} \sum_j \frac{\ell_j}{A_j}$ since $\sigma_2(\omega) \gg \sigma_1(\omega)$ at subgap frequencies. Using London's expression for σ_2 , we get

$$L_k = \mu_0 \lambda^2 \sum_j \frac{\ell_j}{A_j}. \quad (22)$$

We use Eqs. (21) and (22) below for explicit numerical estimates of noise as a function of SC device parameters.

IV. ENERGY DISTRIBUTION FOR QPS IN QUASIEQUILIBRIUM

A recent experiment presented evidence that SC QPs are at thermal equilibrium with the phonon bath, despite their out-of-equilibrium density. In [18] the following empirical expression for the distribution of QPs in SC circuits was proposed,

$$n(E) = x_{\text{QP}} \sqrt{\frac{\Delta}{2\pi k_B T}} e^{-\frac{E-\Delta}{k_B T}}. \quad (23)$$

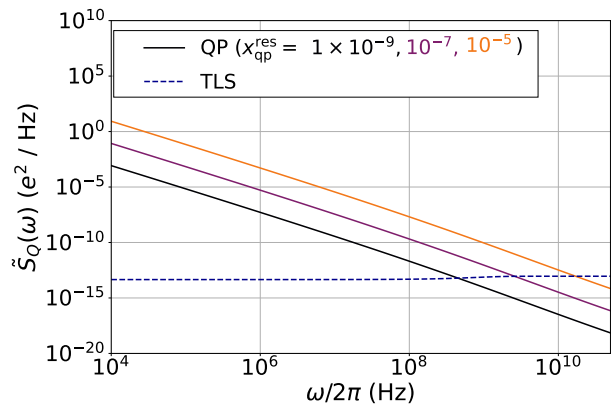


FIG. 2. Charge noise due to quasiequilibrium QPs (solid lines) in the SC aluminum wire forming a CPW resonator for 3 values of $x_{\text{QP}}^{\text{res}}$ ranging from 10^{-9} (black) to 10^{-5} (orange). For comparison, charge noise due to dielectric loss assuming typical loss tangents in bulk and surface is shown (dashed line). Assumed parameters in Table I.

Note that this expression follows the quasithermal law mentioned above; in fact Eq. (23) is a Maxwell-Boltzmann distribution with *out-of-equilibrium chemical potential* $\mu = \Delta$. The fraction of QPs (normalized by the density of Cooper pairs) is modeled as

$$x_{\text{QP}} = x_{\text{QP}}^{\text{res}} + \sqrt{\frac{2\pi k_B T}{\Delta}} e^{-\frac{\Delta}{k_B T}}, \quad (24)$$

so that the first contribution $x_{\text{QP}}^{\text{res}}$ is the fraction of QPs that are out of thermal equilibrium, with the second contribution describing QPs at thermal equilibrium. At high temperatures ($k_B T \geq 100$ mK in [18]), thermal QPs were found to dominate x_{QP} , in that $x_{\text{QP}} \approx \sqrt{2\pi k_B T / \Delta} e^{-\Delta / k_B T}$ leading to $n(E) \approx f(E)$. However, at low temperatures, resident QPs with temperature independent density $x_{\text{QP}}^{\text{res}}$ were found to dominate.

V. NOISE IN QUASIEQUILIBRIUM

A. Charge noise in the SC wire of a CPW

As is shown in Appendix A, the fluctuation-dissipation theorem remains valid for QP energy distributions that satisfy the “quasithermal law” such as Eq. (23). Using Eqs. (5) and (13) we get the charge noise generated by QPs residing in a circuit,

$$\tilde{S}_Q(\omega) = \sum_{\text{disc. wires}} \frac{2\hbar\sigma_1(\omega)}{\omega} \left(\sum_j \frac{\ell_j}{A_j} \right)^{-1} [n_B(\omega) + 1]. \quad (25)$$

At thermal equilibrium ($x_{\text{QP}}^{\text{res}} = 0$) and $k_B T \ll \Delta$, charge noise is exponentially small: E.g. less than 10^{-30} e^2/Hz above 10 MHz for $T = 30$ mK for a typical aluminum

SC CPW (e is the electron's charge). In contrast, Fig. 2 shows the predicted charge noise in an aluminum CPW resonator with one wire segment with $\ell = 20$ mm, $A = 1 \mu\text{m}^2$ and other parameters described in Table I. The assumed resident QP densities of $x_{\text{QP}}^{\text{res}} = 10^{-9} - 10^{-5}$ were previously measured in aluminum qubits, $x_{\text{QP}}^{\text{res}} = 10^{-9} - 10^{-5}$ [14, 18, 29]. We find the QP charge noise is several orders of magnitude larger: E.g. over 20 orders of magnitude larger for $x_{\text{QP}}^{\text{res}} = 10^{-9}$ compared to thermal QPs at 30 mK in the same aluminum device.

Charge noise scales proportional to A/ℓ , showing that it's more important for small wires. This geometric dependence originates from the charge susceptibility being inversely proportional to the wire's impedance. At low frequencies $\hbar\omega \ll k_B T$ and low temperatures $k_B T \ll \Delta$, x_{QP} is independent of T and the charge noise scales as $\tilde{S}_Q(\omega) \propto \ln(4k_B T/\hbar\omega)/(T^{1/2}\omega^2)$. At high frequencies $\tilde{S}_Q(\omega) \propto 1/\omega^{5/2}$ is independent of temperature.

It is illustrative to compare the predicted QP charge noise to Eq. (9), the charge noise due to TLSs in the dielectric materials of the CPW resonator. This is done by including a surface loss tangent in Eq. (10) in order to account for (1) TLSs in the dielectric on the surface of the SC wire forming the center-strip of the CPW (metal-air and metal-substrate interfaces described in [25, 30]), plus (2) the dielectric at the surface of the substrate in the gap between the center-strip and the ground plane (substrate-air interface). In addition, we also included a bulk loss tangent due to TLSs at the substrate. All assumed parameters are described in Table I.

Fig. 2 shows that resident QPs dominate charge noise in CPWs at low frequencies and up to GHz. Only for extremely high frequencies the TLSs become more relevant than QPs. This suggests that noise from resident QPs is particularly relevant at off-resonant frequencies. Note that in Fig. 2 we use ω to indicate a general frequency, not necessarily equal to the resonant frequency Ω .

Several experiments focus on measurements of the loss tangent, extracted either from measurements of qubit relaxation rate [25] or from measurements of the quality factor of resonators [26]. In these cases the contribution from QPs is often intertwined with the one from TLSs. For example, in resonator experiments the QP contribution can be extracted from the part of the quality factor that does not increase with increasing power [26]. Comparing Eqs. (25) and (9) we can express the QP mechanism as a loss tangent,

$$\langle \tan(\delta_{\text{QP}}) \rangle = \frac{A\sigma_1(\omega)}{C\ell^2\omega}, \quad (26)$$

where $C \equiv C/\ell$ is the capacitance per unit length of the CPW. While such an interpretation might be useful for comparison, it must be emphasized that the two mechanisms have fundamentally different origins: Dielectric loss corresponds to electrical energy being absorbed into the excitation of TLSs. In contrast, wire-resident QPs are resistive charge carriers, that turn electrical energy into

heat due to their scattering into impurities and phonons in the SC wire.

B. Quality factor of a CPW resonator

We now quantify how the presence of resident QPs can limit the quality factor Q of a resonator. The quality factor is given by $Q^{-1} = \sum_i Q_i^{-1} + Q_{\text{QP}}^{-1}$, where the contribution due to Ohmic loss from QPs is Q_{QP}^{-1} and the Q_i^{-1} s are contributions from other loss mechanisms. From Eqs. (6) and (13),

$$\frac{1}{Q_{\text{QP}}} = \frac{A}{\ell^2 C \Omega} \sigma_1(\Omega) \coth\left(\frac{\hbar\Omega}{2k_B T}\right), \quad (27)$$

with $\Omega = 1/\sqrt{LC}$. At high frequencies,

$$\frac{1}{Q_{\text{QP}}} \approx \frac{A}{\ell^2 C \mu_0 \lambda^2} x_{\text{QP}} \left(\frac{2\Delta}{\hbar\pi^2 \Omega^5}\right)^{1/2}. \quad (28)$$

We calculate the impact of QPs in Q , Eq. (27), for 3 values of $x_{\text{QP}}^{\text{res}}$ in an aluminum CPW half-wavelength-resonator of length $\ell = \frac{c\pi}{n\Omega}$; c is the speed of light and n the substrate refractive index. We assume $n = \sqrt{11.7}$ (silicon) and fix the characteristic impedance $Z_0 = \sqrt{L/C}$ to 50 Ohms. We compare this to the contribution from dielectric loss due to TLSs with $1/Q_{\text{TLS}} = 3.3 \times 10^{-6}$. Results are shown in Fig. 3. We find that a large density of resident QPs ($x_{\text{QP}}^{\text{res}} \gtrsim 10^{-7}$) can have greater impact in Q than TLSs at resonant frequencies in the GHz range. Assumed parameters shown in Table I.

TABLE I. Device parameters used in figures.

$T=30$ mK, $T_c = 1.2$ K, $\Delta/(2\pi\hbar) = 44$ GHz, $\lambda = 50$ nm (aluminum), $\tan(\delta_{\text{TLS},0}^S) = 1 \times 10^{-3}$, and $\tan(\delta_{\text{TLS},0}^B) = 1 \times 10^{-6}$ in all cases.

	Fig. 2	Fig. 3	Fig. 4	Fig. 5
CPW center-strip (μm)	10	10		10
CPW gap (μm)	6	6		6
ℓ (mm)	20	$\frac{c\pi}{n\Omega}$	0.015	20
A (μm^2)	1	1	0.1	1
p_S ($\times 10^{-4}$) [25, 30]	23	23	2.4	23
p_B [25]	0.9	0.9	0.9	0.9
$\hbar\Omega$		\hbar/\sqrt{LC}	$\sqrt{8E_J E_C} - E_C$	
$Z_0 = \sqrt{L/C}$ (Ohms)		50		
E_J/E_C			70	
C (pF)	3.3	$1/(Z_0\Omega)$	$\sqrt{2e^4 E_J/E_C}/(\hbar\Omega)$	3.3
L (nH)				8.4

C. Relaxation time of a transmon qubit

We now calculate the relaxation rate $1/T_1$ of a transmon. From Eqs. (6) and (13), the contribution due to

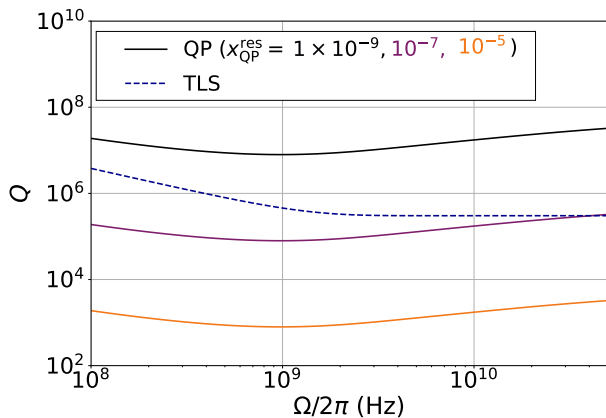


FIG. 3. Quality factor due to quasiequilibrium QPs (solid lines) in an aluminum CPW resonator for 3 values of $x_{\text{QP}}^{\text{res}}$ ranging from 10^{-9} (black) to 10^{-5} (orange). The length of the resonator is adjusted to match the resonance frequency Ω for the fundamental mode, $\ell = \frac{c\pi}{n\Omega}$. For comparison, we include the Q due to dielectric loss with typical loss tangents in bulk and surface (dashed line). Other parameters in Table I.

Ohmic loss from QPs is given by

$$\frac{1}{T_1^{\text{QP}}} = \sum_{\text{disc. wires}} \frac{\sigma_1(\Omega)}{C} \left(\sum_j \frac{\ell_j}{A_j} \right)^{-1} \coth \left(\frac{\hbar\Omega}{2k_B T} \right), \quad (29)$$

where $\hbar\Omega = \sqrt{8E_C E_J} - E_C$, and the sum extends over all SC wire segments forming the transmon. For most transmons the sum is dominated by the lead regions connecting the Josephson junction to the large pad electrodes. For example, the transmons fabricated in [25] have ℓ/A for the pad and lead regions equal to $500 \mu\text{m}/(25\mu\text{m}^2) = 20/\mu\text{m}$, and $15 \mu\text{m}/(0.1\mu\text{m}^2) = 150/\mu\text{m}$, respectively (we assumed the SC film thickness is $0.1 \mu\text{m}$). As a result the lead region dominates the geometric dependence of $1/T_1^{\text{QP}}$. At high frequencies and assuming the lead region dominates we get

$$\frac{1}{T_1^{\text{QP}}} \approx \frac{2x_{\text{QP}}}{C\mu_0\lambda^2} \left(\text{Max} \left\{ \frac{\ell}{A} \right\} \right)^{-1} \left(\frac{2\Delta}{\hbar\pi^2\Omega^3} \right)^{1/2}, \quad (30)$$

with the factor of 2 accounting for the two disconnected wires forming the transmon. We calculate Eq. (29) for 3 different values of $x_{\text{QP}}^{\text{res}}$ in an aluminum transmon qubit and compare it to the contribution from dielectric loss due to TLSs. For this, we fix the ratio $E_J/E_C = 70$ and consider only the small leads near the transmon's junction, other parameters shown in Table I. For comparison, we plot $T_1^{\text{QP (junction)}}$, arising from QPs tunneling through a Josephson junction *without gap asymmetry* [10, 11]:

$$\frac{1}{T_1^{\text{QP (junction)}}} = x_{\text{QP}} \left(\frac{2\Delta\Omega}{\hbar\pi^2} \right)^{1/2}, \quad (31)$$

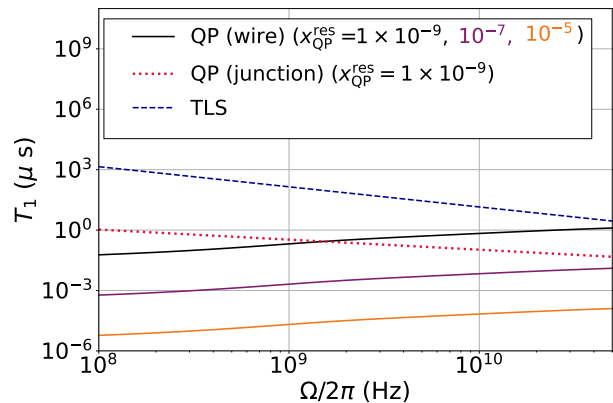


FIG. 4. Relaxation time due to quasiequilibrium QPs (solid lines) in an aluminum transmon for 3 values of $x_{\text{QP}}^{\text{res}}$ ranging from 10^{-9} (black) to 10^{-5} (orange). For comparison, T_1 due to dielectric loss assuming typical loss tangents in bulk and surface (dashed line) and T_1 due to QP-tunneling in symmetric junctions for $x_{\text{QP}}^{\text{res}} = 10^{-9}$ (dotted line) are shown. Assumed parameters are included in Table I.

valid at high frequencies. Figure 4 shows that Ohmic loss from QPs may give a larger contribution to the relaxation rate than both the TLS and the QP tunneling mechanisms.

D. Flux noise

As explained in the end of Section II, there is flux noise spectral density associated to charge noise, as in $\tilde{S}_\Phi(\omega) = (L\omega)^2 \tilde{S}_Q(\omega)$. The associated flux noise due to resident QPs is then

$$\tilde{S}_\Phi(\omega) = 2\hbar\omega \sum_{\text{disc. wires}} L^2 \sigma_1(\omega) \left(\sum_j \frac{\ell_j}{A_j} \right)^{-1} [n_B(\omega) + 1], \quad (32)$$

where L is the effective inductance for each disconnected wire. Note how the geometric dependence is different from charge noise. For example, a single CPW wire with constant inductance per unit length will have Eq. (32) directly proportional to wire length ℓ , the opposite behavior of charge noise Eq. (25). At low frequencies ($\hbar\omega \ll k_B T$), flux noise scales logarithmically with frequency and temperature, $\tilde{S}_\Phi(\omega) \propto \ln(4k_B T/\hbar\omega)/T^{1/2}$. For not too wide frequency bands this will appear as “nearly white” flux noise. In contrast, for $\hbar\omega \gg k_B T$, $\tilde{S}_\Phi(\omega) \propto 1/\sqrt{\omega}$.

Luthi et al. [23] observed a white flux noise background of magnitude $3.6 \times 10^{-15} \Phi_0^2/\text{Hz}$ of unknown origin in a NbTiN Superconducting Quantum Interference Device (SQUID). Another experiment performed in a different device of the same material measured a similar white flux noise background of magnitude $2 \times 10^{-16} \Phi_0^2/\text{Hz}$ [31]. Can our proposed QP mechanism explain the origin of

this white flux noise background? To try to answer this question, we use our Eq. (32) to estimate the required $x_{\text{QP}}^{\text{res}}$ that yields the noise level observed in these experiments. From Eq. (22), we estimate a value of kinetic inductance per unit length of the order of 100 nH/m for these devices. Assuming $\mathcal{L} \approx \mathcal{L}_k$ and other parameters as in [32], we find that $x_{\text{QP}}^{\text{res}} \sim 10^{-3}$ in Eq. (32) would explain the white flux noise background obtained in both experiments [23, 31].

To our knowledge, $x_{\text{QP}}^{\text{res}}$ has not yet been measured in NbTiN devices. Instead, an experiment performed in a NbTi resonator measured $x_{\text{QP}}^{\text{res}} \approx 7 \times 10^{-6}$ [33]. It's important to note that the QP density depends not only on the material but also on the specific sources driving the electron gas out of equilibrium. Also note that a large geometric inductance, not considered in our calculation, would greatly reduce the estimated $x_{\text{QP}}^{\text{res}}$. Therefore, a measurement of $x_{\text{QP}}^{\text{res}}$ in these devices is needed before reaching a definite conclusion.

To quantify the flux noise contribution due to resident quasithermal QPs, we compare it to the flux noise generated by bulk and surface TLSs,

$$\begin{aligned} \tilde{S}_{\Phi}^{\text{TLS}}(\omega) &= (L\omega)^2 \tilde{S}_Q^{\text{TLS}}(\omega) \\ &= 2\hbar L^2 \omega^2 C \langle \tan(\delta_{\text{TLS}}) \rangle [n_B(\omega) + 1]. \end{aligned} \quad (33)$$

Figure 5 shows this comparison in an aluminum CPW, for the same parameters assumed in Fig. 2, plus inductance per unit length $\mathcal{L} = 420$ nH/m. Figure 5 also shows the spin-impurity contribution $\tilde{S}_{\Phi}^{\text{spins}}(\omega) = 2\pi \times 10^{-9} \Phi_0^2/\omega$, which is the value expected from a CPW with $\ell = 20$ mm, that is 10 \times larger than [22].

For $x_{\text{QP}}^{\text{res}} = 10^{-9}$, our predicted amplitude of the “nearly white” flux noise background due to QP Ohmic loss is of the same order of magnitude as the amplitude measured in flux noise experiments by Quintana *et al.* [22], in the 10 – 1000 MHz band with aluminum devices of similar dimension as in Fig. 5. Quintana *et al.* [22] measured a flux noise frequency dependence that changed from $1/\omega$ at low frequency to ω^m with exponent $m = 1-3$ at large frequencies. This frequency dependence can not be explained by the present QP mechanism. The low frequency $1/\omega$ contribution can be explained by spin impurities [7], while the high frequency “superOhmic” contribution remains unexplained.

Here we point out that the flux noise associated to TLS charge noise may provide an explanation for the superOhmic noise measured in [22]. As we see in Eq. (33), $\tilde{S}_{\Phi}^{\text{TLS}}(\omega)$ is proportional to ω^2 in the low T regime. A TLS loss tangent of $\langle \tan(\delta_{\text{TLS}}) \rangle = 10^{-6} - 10^{-5}$ would match the superOhmic flux noise measured by Quintana *et al.* with superOhmic exponent $m = 2$.

VI. CONCLUSIONS

In conclusion, we presented a theoretical model of charge and flux noise due to Ohmic loss from resident

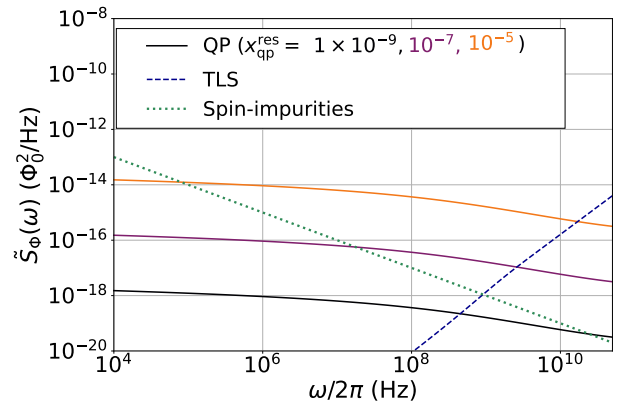


FIG. 5. Flux noise due to quasiequilibrium QPs (solid lines) in an aluminum CPW resonator with $\ell = 20$ mm for 3 values of $x_{\text{QP}}^{\text{res}}$ ranging from $= 10^{-9}$ (black) to 10^{-5} (orange). For comparison, flux noise due to dielectric loss (dashed) and spin impurities (dotted) is included. The former assumes typical TLS loss tangents/participation ratios in bulk and surface, and the latter is 10 \times the impurity-spin flux noise measured in a wire with $\ell \approx 2$ mm [22]. Assumed parameters are shown in Table I.

QPs in SC wires valid for resident QP energy distributions. By assuming a quasithermal distribution validated by experimental observations, we estimated the impact of charge and flux noise generated by this mechanism. We found that resident QPs in a SC wire can contribute more to charge noise than dielectric loss generated by TLSs at low frequencies and up to GHz. This conclusion might appear surprising given that several experiments concluded that $T_2 \approx 2T_1$ and TLSs dominate $1/T_1$ in transmons. But as it turns out, these experiments often take advantage of techniques to dramatically reduce QP population in their devices. For example, in [25] it was mentioned that shielding plus cooling with an external magnetic field was used to reduce QP generation and increase QP recombination before data was taken (See endnote 21 in [25]).

This dominance of QP Ohmic loss over TLSs at non-resonant low frequencies shows that this mechanism gives an important contribution to qubit phase fluctuation, increasing $1/T_2$ beyond its energy relaxation floor $1/(2T_1)$. This contribution will become more important as losses from surface TLSs continue to be reduced by better materials and circuit designs [34, 35].

We also show that the impact of Ohmic loss due to QPs in the quality factor of resonators can be larger than dielectric loss due to TLSs. Similarly, transmon relaxation times T_1 can be significantly limited by this mechanism. We find that Ohmic loss from resident QPs can even be larger than loss from QPs tunneling through symmetric junctions, often believed to be the main source of energy relaxation in these devices. The geometric dependence of QP Ohmic loss in SC wires shows that this effect can be mitigated by making compound wires with high impedance regions, i.e. sections with large ℓ/A . This is

indeed the case for transmons, that have small leads near their junction [25, 36].

As explained in section II, charge noise in an inductive element can also be interpreted as flux noise. This is particularly important in cases where flux noise is extracted from $1/T_1$ measurements, as this flux noise can originate from charge fluctuations. We find that charge noise from resident QP densities is equivalent to a nearly-white flux noise background. This provides a possible explanation for the noise background observed in NbTiN devices [23, 31], although additional measurements are needed before a definite conclusion is established. The magnitude of flux noise predicted by our model is comparable to $1/\omega$ flux noise levels measured in other devices in the 10 – 1000 MHz band [22], suggesting the importance of this mechanism as the presence of spin impurities is mitigated [37]. Furthermore, we argued that TLSs are a source of superOhmic flux noise at high frequencies. This contribution can potentially explain the origin of superOhmic flux noise in the GHz range [22].

In conclusion, out-of-equilibrium QPs are shown to be an important source of charge and flux noise even when the QPs reside away from Josephson junctions. Depending on the magnitude of QP density, the associated noise amplitudes might be larger than those arising from amorphous TLSs and spin impurities.

Appendix A: Fluctuation-Dissipation Theorem for quasiequilibrium distributions

This appendix presents a generalized formulation of the fluctuation-dissipation theorem that shows that it remains valid for quasithermal distributions such as Eq. (23).

Assume a system described by a Hamiltonian \mathcal{H}_0 is perturbed by an external Hamiltonian $\mathcal{H}_{\text{ext}} = -F(t)\hat{O}$ with \hat{O} an observable of interest coupled to its conjugate field $F(t)$. The *susceptibility operator* $\hat{\chi}_O$ is defined according to linear-response theory: $\hat{O}_{F \neq 0}(t) - \hat{O}_{F=0}(t) = \int_{-\infty}^{\infty} dt' \hat{\chi}_O(t-t')F(t')$. From time-dependent perturbation theory we get $\hat{\chi}_O(t-t') = \frac{i}{\hbar}\theta(t-t')[\hat{O}(t), \hat{O}(t')]$, where $\hat{O}(t) = e^{i\mathcal{H}_0 t/\hbar} O e^{-i\mathcal{H}_0 t/\hbar}$ is the observable in the interaction picture. In Fourier space we get $\delta\hat{O}(\omega) = \hat{\chi}_O(\omega)\delta\tilde{F}(\omega)$, with susceptibility operator given by

$$\hat{\chi}_O(\omega) = \frac{1}{2\pi\hbar} \int_{-\infty}^{\infty} d\omega' \frac{[\hat{S}_O(-\omega')]^\dagger - \hat{S}_O(\omega')}{\omega - \omega' + i\eta}, \quad (\text{A1})$$

where $\hat{S}_O(t) = [\hat{O}(t) - \langle\hat{O}(0)\rangle_{\hat{\rho}}][\hat{O}(0) - \langle\hat{O}(0)\rangle_{\hat{\rho}}]$ is the *cor-*

relation operator, $\hat{S}_O(\omega) = \int_{-\infty}^{\infty} dt e^{i\omega t} \hat{S}_O(t)$ is its Fourier transform and $\langle\hat{O}(0)\rangle_{\hat{\rho}} = \text{Tr}\{\hat{\rho}\hat{O}(0)\}$ is the average of $\hat{O}(0)$ at a state described by an arbitrary density matrix $\hat{\rho}$.

Equation A1 is an exact operator identity. We now specialize to the case where the system is described by a density matrix that is (1) independent of time (i.e. in a steady state) and (2) diagonal in the basis formed by the energy eigenstates $\{|E\rangle\}$ of \mathcal{H}_0 : $\langle E|\hat{\rho}|E'\rangle = \rho(E)\delta_{E,E'}$ with $\rho(E)$ a real function. Take the average of Eq. (A1) in a such a state and separate its imaginary part to get a *more general version* of the fluctuation-dissipation theorem:

$$2\hbar\text{Im}\left\{\langle\hat{\chi}_O(\omega)\rangle_{\rho(E)}\right\} = \langle\hat{S}_O(\omega)\rangle_{\rho(E)} - \langle\hat{S}_O(\omega)\rangle_{\rho(E+\hbar\omega)}. \quad (\text{A2})$$

This is based on the identity $\langle[\hat{S}_O(-\omega')]^\dagger\rangle_{\rho(E)} = \langle\hat{S}_O(\omega)\rangle_{\rho(E+\hbar\omega)}$, that is valid for a density matrix that satisfies the conditions (1) and (2) above. Note that in Eq. (A2) the quantities $\langle\hat{\chi}_O(\omega)\rangle_{\rho(E)}$ and $\langle\hat{S}_O(\omega)\rangle_{\rho(E)}$ are the usual susceptibility and power spectral density of \hat{O} , respectively; the notation makes their dependence on $\rho(E)$ explicit.

When $\hat{\rho}$ satisfies the “quasithermal law” $\hat{\rho} \propto e^{-\mathcal{H}/k_B T}$ we get $\rho(E + \hbar\omega) = e^{-\hbar\omega/k_B T}\rho(E)$. This implies $\langle\hat{S}_O(\omega)\rangle_{\rho(E+\hbar\omega)} = e^{-\hbar\omega/k_B T}\langle\hat{S}_O(\omega)\rangle_{\rho(E)}$, leading to the usual fluctuation-dissipation theorem:

$$\langle\hat{S}_O(\omega)\rangle_{\rho(E)} = 2\hbar\text{Im}\left\{\langle\hat{\chi}_O(\omega)\rangle_{\rho(E)}\right\}[n_B(\omega) + 1], \quad (\text{A3})$$

where $n_B(\omega)$ is the Bose-Einstein distribution. Therefore, the usual fluctuation-dissipation theorem holds for a quasithermal distribution.

ACKNOWLEDGMENTS

We wish to thank the Engineering Quantum Systems group led by W.D. Oliver at the Massachusetts Institute of Technology for hosting Nava Aquino during part of this work. We acknowledge encouragement and useful discussions with M. Amin, W. A. Coish, M. Hays, P. Kovtun, T. Lanting, W. D. Oliver, K. Serniak, and T. Stavenga. This work was supported by the Natural Sciences and Engineering Research Council of Canada (NSERC) through its Discovery (RGPIN-2020-04328), and its Alliance International Catalyst Quantum Grant (ALLRP-586318-23).

-
- [1] J. Clarke and F. Wilhelm, Superconducting quantum bits, *Nature* **453**, 1031 (2008).
 [2] J. M. Martinis *et al.*, Decoherence in josephson qubits

- from dielectric loss, *Phys. Rev. Lett.* **95**, 210503 (2005).
 [3] R. H. Koch, D. P. DiVincenzo, and J. Clarke, Model for $1/f$ flux noise in squids and qubits, *Phys. Rev. Lett.* **98**,

- 267003 (2007).
- [4] S. Sendelbach, D. Hover, A. Kittel, M. Mück, J. M. Martinis, and R. McDermott, Magnetism in squids at millikelvin temperatures, *Phys. Rev. Lett.* **100**, 227006 (2008).
- [5] J. Gao *et al.*, A semiempirical model for two-level system noise in superconducting microresonators, *Appl. Phys. Lett.* **92**, 212504 (2008).
- [6] T. Lanting, M. H. Amin, A. J. Berkley, C. Rich, S.-F. Chen, S. LaForest, and R. de Sousa, Evidence for temperature-dependent spin diffusion as a mechanism of intrinsic flux noise in squids, *Phys. Rev. B* **89**, 014503 (2014).
- [7] J. A. Nava Aquino and R. de Sousa, Flux noise in disordered spin systems, *Phys. Rev. B* **106**, 144506 (2022).
- [8] D. C. Mattis and J. Bardeen, Theory of the anomalous skin effect in normal and superconducting metals, *Phys. Rev.* **111**, 412 (1958).
- [9] R. M. Lutchyn, L. I. Glazman, and A. I. Larkin, Kinetics of the superconducting charge qubit in the presence of a quasiparticle, *Phys. Rev. B* **74**, 064515 (2006).
- [10] J. M. Martinis, M. Ansmann, and J. Aumentado, Energy decay in superconducting josephson-junction qubits from nonequilibrium quasiparticle excitations, *Phys. Rev. Lett.* **103**, 097002 (2009).
- [11] G. Catelani, R. J. Schoelkopf, M. H. Devoret, and L. I. Glazman, Relaxation and frequency shifts induced by quasiparticles in superconducting qubits, *Phys. Rev. B* **84**, 064517 (2011).
- [12] G. Catelani, J. Koch, L. Frunzio, R. J. Schoelkopf, M. H. Devoret, and L. I. Glazman, Quasiparticle relaxation of superconducting qubits in the presence of flux, *Phys. Rev. Lett.* **106**, 077002 (2011).
- [13] J. Aumentado, M. W. Keller, J. M. Martinis, and M. H. Devoret, Nonequilibrium quasiparticles and $2e$ periodicity in single-cooper-pair transistors, *Phys. Rev. Lett.* **92**, 066802 (2004).
- [14] K. Serniak, M. Hays, G. de Lange, S. Diamond, S. Shankar, L. D. Burkhardt, L. Frunzio, M. Houzet, and M. H. Devoret, Hot nonequilibrium quasiparticles in transmon qubits, *Phys. Rev. Lett.* **121**, 157701 (2018).
- [15] A. Vepsäläinen, A. Karamlou, J. Orrell, *et al.*, Impact of ionizing radiation on superconducting qubit coherence, *Nature* **584**, 551 (2020).
- [16] S. Diamond, V. Fatemi, M. Hays, H. Nho, P. D. Kurilovich, T. Connolly, V. R. Joshi, K. Serniak, L. Frunzio, L. I. Glazman, and M. H. Devoret, Distinguishing parity-switching mechanisms in a superconducting qubit, *PRX Quantum* **3**, 040304 (2022).
- [17] P. Du, D. Egana-Ugrinovic, R. Essig, and M. Sholapurkar, Sources of low-energy events in low-threshold dark-matter and neutrino detectors, *Phys. Rev. X* **12**, 011009 (2022).
- [18] T. Connolly, P. D. Kurilovich, S. Diamond, H. Nho, C. G. L. Böttcher, L. I. Glazman, V. Fatemi, and M. H. Devoret, Coexistence of nonequilibrium density and equilibrium energy distribution of quasiparticles in a superconducting qubit, *Phys. Rev. Lett.* **132**, 217001 (2024).
- [19] T. Yamamoto, Y. Nakamura, Y. A. Pashkin, O. Astafiev, and J. S. Tsai, Parity effect in superconducting aluminum single electron transistors with spatial gap profile controlled by film thickness, *Applied Physics Letters* **88**, 212509 (2006).
- [20] G. Marchegiani, L. Amico, and G. Catelani, Quasiparticles in superconducting qubits with asymmetric junctions, *PRX Quantum* **3**, 040338 (2022).
- [21] M. McEwen, K. C. Miao, J. Atalaya, A. Bilmes, A. Crook, J. Bovaird, J. M. Kreikebaum, N. Zobrist, E. Jeffrey, B. Ying, A. Bengtsson, H.-S. Chang, A. Dunsworth, J. Kelly, Y. Zhang, E. Forati, R. Acharya, J. Iveland, W. Liu, S. Kim, B. Burkett, A. Megrant, Y. Chen, C. Neill, D. Sank, M. Devoret, and A. Opremcak, *Resisting high-energy impact events through gap engineering in superconducting qubit arrays* (2024), arXiv:2402.15644 [quant-ph].
- [22] C. M. Quintana, Y. Chen, D. Sank, A. G. Petukhov, T. C. White, D. Kafri, B. Chiaro, A. Megrant, R. Barends, B. Campbell, Z. Chen, A. Dunsworth, A. G. Fowler, R. Graff, E. Jeffrey, J. Kelly, E. Lucero, J. Y. Mutus, M. Neeley, C. Neill, P. J. J. O'Malley, P. Roushan, A. Shabani, V. N. Smelyanskiy, A. Vainsencher, J. Wenner, H. Neven, and J. M. Martinis, Observation of classical-quantum crossover of $1/f$ flux noise and its paramagnetic temperature dependence, *Phys. Rev. Lett.* **118**, 057702 (2017).
- [23] F. Luthi, T. Stavenga, O. W. Enzing, A. Bruno, C. Dickel, N. K. Langford, M. A. Rol, T. S. Jespersen, J. Nygård, P. Krogstrup, and L. DiCarlo, Evolution of nanowire transmon qubits and their coherence in a magnetic field, *Phys. Rev. Lett.* **120**, 100502 (2018).
- [24] R. de Sousa, Electron spin as a spectrometer of nuclear-spin noise and other fluctuations, in *Electron Spin Resonance and Related Phenomena in Low-Dimensional Structures*, edited by M. Fanciulli (Springer, Berlin, Germany, 2009) p. 183.
- [25] C. Wang, C. Axline, Y. Y. Gao, T. Brecht, Y. Chu, L. Frunzio, M. H. Devoret, and R. J. Schoelkopf, Surface participation and dielectric loss in superconducting qubits, *Appl. Phys. Lett.* **107**, 162601 (2015).
- [26] N. Gorgichuk, T. Junginger, and R. de Sousa, Modeling Dielectric Loss in Superconducting Resonators : Evidence for Interacting Atomic Two-Level Systems at the Nb /Oxide Interface, *Phys. Rev. Appl.* **19**, 024006 (2023).
- [27] J. Gao, *The Physics of Superconducting Microwave Resonators*, Ph.D. thesis, California Institute of Technology (2008).
- [28] T. Hong, K. Choi, K. Ik Sim, T. Ha, B. Cheol Park, H. Yamamori, and J. Hoon Kim, Terahertz electro-dynamics and superconducting energy gap of NbTiN, *Journal of Applied Physics* **114**, 243905 (2013).
- [29] P. J. de Visser, J. J. A. Baselmans, P. Diener, S. J. C. Yates, A. Endo, and T. M. Klapwijk, Number fluctuations of sparse quasiparticles in a superconductor, *Phys. Rev. Lett.* **106**, 167004 (2011).
- [30] C. E. Murray, Analytical modeling of participation reduction in superconducting coplanar resonator and qubit designs through substrate trenching, *IEEE Transactions on Microwave Theory and Techniques* **68**, 3263 (2020).
- [31] T. Stavenga, *Flux noise in a magnetic field*, Dissertation (tu delft), Delft University of Technology (2023).
- [32] For this calculation, we assume a mixing chamber temperature of $T=30$ mK. $T_c = 14.1$ K, $\lambda = 260$ nm for NbTiN [28]. The normal state conductivity σ_N is calculated from Eq. (21). For the device in [23], the wire's length is $\ell \approx 100$ μm , the width $W \approx 5$ μm , and the thickness $b \approx 100$ nm. For the device in [31], the wire's length is $\ell \approx 30$ μm , the width $W \approx 2$ μm , and the thickness $b \approx 100$ nm.

- [33] R. Barends *et al.*, Minimizing quasiparticle generation from stray infrared light in superconducting quantum circuits, [Appl. Phys. Lett.](#) **99**, 113507 (2011).
- [34] A. P. M. Place, L. V. H. Rodgers, P. Mundada, *et al.*, New material platform for superconducting transmon qubits with coherence times exceeding 0.3 milliseconds, [Nat Commun](#) **12**, 1779 (2021).
- [35] J. M. Martinis, Surface loss calculations and design of a superconducting transmon qubit with tapered wiring, [npj Quantum Inf](#) **8**, 26 (2022).
- [36] H. Paik, D. I. Schuster, L. S. Bishop, G. Kirchmair, G. Catelani, A. P. Sears, B. R. Johnson, M. J. Reagor, L. Frunzio, L. I. Glazman, S. M. Girvin, M. H. Devoret, and R. J. Schoelkopf, Observation of high coherence in josephson junction qubits measured in a three-dimensional circuit qed architecture, [Phys. Rev. Lett.](#) **107**, 240501 (2011).
- [37] P. Kumar, S. Sendelbach, M. A. Beck, J. W. Freeland, Z. Wang, H. Wang, C. C. Yu, R. Q. Wu, D. P. Pappas, and R. McDermott, Origin and reduction of $1/f$ magnetic flux noise in superconducting devices, [Phys. Rev. Appl.](#) **6**, 041001 (2016).